Effects of surface viscoelasticity on cellular responses of endothelial cells

Motahare-Sadat Hosseini[1], Ali Asghar Katbab*[1]

Abstract

Background: One area of nanoscience deals with nanoscopic interactions between nanostructured materials and biological systems. To elucidate the effects of the substrate surface morphology and viscoelasticity on cell proliferation, fractal analysis was performed on endothelial cells cultured on nanocomposite samples based on silicone rubber (SR) and various concentrations of organomodified nanoclay (OC).

Methods: The nanoclay/SR ratio was tailored to enhance cell behavior via changes in sample substrate surface roughness and viscoelasticity.

Results: Surface roughness of the cured SR filled with negatively-charged nanosilicate layers had a greater effect than elasticity on cell growth. The surface roughness of SR nanocomposite samples increased with increasing the OC content, leading to enhanced cell growth and extracellular matrix (ECM) remodeling. This was consistent with the decrease in SR segmental motions and damping factor as the primary viscoelastic parameters by the nanosilicate layers with increasing clay concentrations.

Conclusions: The inclusion of clay nanolayers affected the growth and behavior of endothelial cells on microtextured SR.

Keywords: Silicone rubber; Nanoclay; Elastic Modulus; Roughness; Cell proliferation

Introduction

In tissue engineering, a growing body of research deals with the improvement of substrates to enhance cell functionality for in vivo applications. The cell-substrate interaction necessitates enhanced material properties to influence cell characteristics including proliferation, morphology, cytoskeletal structure, and differentiation. Physico-mechanical properties of substrates have been shown to influence cell behavior (1, 2). Such properties have been manipulated and modified by changing chemical crosslinking factors (3, 4) or surface topography (5). Chun-Min Lo *et al.* cultured 3T3 fibroblast cells on flexible polyacrylamide sheets and studied the effects of surface rigidity changes on cell migration and spreading (6). Substrate flexibility was altered by bis-acrylamide as a crosslinking agent (6). Guo *et al.* similarly created a polyacrylamide network by adding bis-acrylamide to achieve substrates with

different elastic moduli to demonstrate that tissue regeneration is markedly influenced by matrix surface rigidity (7). Subsequently, substrates made of polystyrene with local micropillars were prepared to investigate cell migration and morphology in response to changes in surface topography (8). Correspondingly, the influence of matrix mechanical properties on glioma cells and neural stem cells were examined (9, 10).

The physicochemical nature of the extracellular matrix (ECM) (10) and selective junctions of trans-membrane proteins such as integrins (11) enables cells to sense and react to stimuli in their environment and initiate a limited repertoire of cellular signals.

The sensitivity of cells arises from the mechanosensitive nature of cell adhesion (12). Cell-matrix adhesion includes dense protein networks (13) in which chemical signaling plays key roles (14).

1: Polymer Engineering and Color Technology Department (Center of Excellence), Amirkabir University of Technology, Tehran, Iran
*Corresponding author: Ali Asghar Katbab; Tel: +98 2164542433; Fax: +98 2164542433; E-mail: katbab@aut.ac.ir

Cytoskeletal arrangement and orientation are highly dependent upon mechanical and structural properties of the matrix such as elastic modulus, Poisson's ratio, and roughness (15, 16). For example, a substrate displays different behaviors in response to cell aggregation according to its physical and mechanical properties (17). In other words, if a substrate is stiff and non-elastic, focal adhesions serve as structural links between the ECM and the actin cytoskeleton (7). Focal adhesion is a stable contact that mediates cell adhesion to the substrate (18). In contrast, soft and elastic substrates provide transient cell-matrix anchoring (19).

When interacting with the substrate, cellular responses. including relaxation time and adaptation by alterations in fibrous structures, are defined by local matrix deformability (20, 21). The adjustment of the cell cytoskeleton to the substrate's mechanical properties depends on polymerization and depolymerization of actin fibers (22), which act via focal adhesion proteins at the cell-substrate interface (20). In the current study, a silicone rubber (SR) -based substrate was modified by the inclusion of different mass ratios of organomodified-nanoclay (OC) particles. The resultant surface properties were evaluated and the effects of alterations in surface viscoelastic properties on cell behavior are described.

Materials and Methods

Preparation of nanocomposites

Medical grade HTV silicone rubber manufactured by Dow Corning (USA) was used as the base material. Nanocomposites were prepared using Organoclay grade Closite 15A (Southern Clay Products, USA). Nanocomposite samples were prepared via a melt-mixing process using a Brabender Plasti-Corder PL2000 Brabender (USA) in 60 cc with a mixing rate of 60 rpm at 60 °C for 20 minutes. Dicumyl peroxide (95%) as crosslinking agent was added to the compound during the mixing on a laboratory-sized two-roll mixer (Farrel Bridge LTD, UK) at 60 °C (4). The prepared compounds were vulcanized at 160 °C by compression molding for 9 min as the optimum cure time.

Evaluation of mechanical properties

The mechanical properties, including elastic modulus at tension and elongation at break, were determined using a tensile testing device (Cardano al Campo (VA), Italy). Samples were prepared and tested according to the standard ASTM D412 protocol (23).

Dynamic mechanical analysis

The solid viscoelastic behavior of the cross-linked samples was evaluated by measuring the storage modulus (E') and the dynamic mechanical loss factor (tan δ = E''/E') using a dynamic thermal mechanical analyzer (DMTA; model 2980 V 1.7B, Germany). The samples were analyzed in the tension mode at a constant frequency of 1 Hz, and a heating rate of 5 °C/min over a temperature range of -160 to 50 °C. A decrease in the storage modulus versus time curve indicated relaxation. The temperature corresponding to the peak in tan δ versus temperature was defined as the glass–rubber transition temperature (T_g) (24).

Atomic force microscopy (AFM)

The effects of organomodified silicate clay layers on the morphology and topology of the cured SR and corresponding nanocomposites were assessed by atomic force microscopy (MultiMode AFMTM from Digital Instruments, Santa Barbara, CA, USA) on the sample surfaces. For each sample, three topographic images were recorded and the related surface profiles were analyzed using nanoscope image processing software (Q-Scope). Phase images were captured on 5×5 μm areas from with average heights less than 0.5 μm with a 2 Hz scan rate and 400 samples per line resolution (25, 26).

Cell culture

Human umbilical vein endothelial cells (HUVECs) were cultured in DMEM + Ham's F12 (Gibco, USA) containing 10% fetal bovine serum (FBS) (Seromed, Germany) and incubated in 5% CO_2 at 37 °C. Silicone nanocomposite substrates were coated by collagen type I (Sigma, USA) at 0.5 mg/mL for proper cell attachment. The confluent cells were transferred to the coated substrates and incubated overnight, after which cell images were captured and processed.

Cell counting and morphology

The images were captured via an inverted microscope (Zeiss, Germany) after 24 hours and analyzed using the MATLAB-based image analysis code (TheMathWorks, Inc., USA) to approximate topological and fractal dimension (FD) parameters (27).

To evaluate cell growth, the area covered by the cells in each image was determined and the ratio of cell-to-total area was determined by producing binary

images and segregating the cells from the background. The cell density was determined by calculating the number of adherent cells and comparing that to the number of cells in the initial culture. To quantify alterations in cell morphologies, the average shape index (SI), an objective metric of elongation, and average orientation angle (ɵ) were determined. The ɵ parameter was defined by the angle between the longitudinal axis of the cell and the shortest line to the nearest cell (15, 28).

Zymogram analysis for promatrix metalloproteinase-2 (PMMP-2) secreted by HUVECs
A 72 kDa gelatinase activity from tissue culture supernatants was assayed using polyacrylamide-gelatin zymography. Briefly, 10 µl from each sample were mixed with an equal volume of non-reducing sample buffer and electrophoresed on 10% polyacrylamide gels containing 0.1% gelatin. Samples were electrophoresed at 10 mA for 1.5 h at 4 °C.

To regain PMMP-2 activity by eliminating sodium dodecyl sulfate (SDS) remnants, gels were washed in 2.5% Triton-X-100 three times for 30 min at room temperature. Washed gels were bathed in proteolysis (activation) buffer (10 mM $CaCl_2$, 0.1 mM Tris-HCl,

pH 7.4) and incubated overnight at 37 °C. Gels were then rinsed in 2.5% Triton-X-100 and stained at room temperature with 0.05% Coomassie Brilliant Blue-250 (30% methanol, 60% H_2O, 10% acetic acid) for 1 h on a rotator. Gels were then de-stained in 20% methanol/10% acetic acid until color-free bands, indicating proteolytic activity, were distinguishable from the Coomassie blue-stained background (29).

Statistics
The data were analyzed by the *t*-test. Data was presented as mean values ± S.D. and $p < 0.05$ was considered statistically significant.

Results
Mechanical properties
Table 1 summarizes the mechanical properties and roughness factor values for the cross-linked neat SR and corresponding nanocomposites. Results indicated increasing matrix stiffness as the concentration of the nanoparticles was increased (*p < 0.05*). An increase of 18% was observed in the tensile modulus when the mass ratio of the nanoparticles was increased from 0 to 3%.

Table 1. Mechanical properties and roughness factor for cured neat SR and corresponding nanocomposites

Sample	E (N/mm^2)	Elongation at break (%)	R_{rms} (nm)	R_a (nm)
SR	1.47±0.08	356.19±26.72	14.69±0.46	11.44±0.18
SR-OC (1%)	1.49±0.19	353.55±33.53	21.43±0.33	16.68±0.54
SR-OC (2%)	1.57±0.09	340.59±25.02	22.02±0.42	16.90±0.68
SR-OC (3%)	1.73±0.06	289.04±14.30	43.16±1.82	29.56±8.04

Viscoelastic behavior of SR-OC bionanocomposites
The effect of the incorporation of organically-modified Closite 15A particles on the viscoelastic behavior of the cured SR compounds was assessed by DMTA. The storage modulus as a function of temperature, as well as values of the measured thermophysical parameters (T_g and melting temperature) and loss factor (tan δ), are shown in Figure 1 and Table 2, respectively.

The value of the storage modulus for samples decreased as the temperature increased due to the increase in the mobility of molecular chains (Fig. 1). The sharp decrease in the storage modulus is observed near the glass transition temperature.

The silicone elastomer exhibited two peaks in the tan δ plot over the temperature range studied. The low temperature peak is at a glass transition temperature

and not dramatic. The higher temperature peak corresponds to a crystalline melting point. The melting point of the pure and reinforced silicone was only slightly affected by increasing the OC filler content in the SR matrix (Table 2). However, increasing the OC filler content increased the T_g relative to that of SR alone. The T_g values of the neat SR, and 1, 2, and 3 wt% of nanoclay were -113.0, -99.3, -90.5, and -81.1 °C, respectively. The T_g's of the nanocomposites were higher than that of the neat polymer. The addition of clay platelets caused an increase in the T_g consistent with the hindered action of nanoclay particles (30). The maximum tan δ height for neat and nanocomposites was reduced as the nanofiller concentration increased. The maximum tan δ values for neat polymer, and 1, 2, and 3% nanoclay-loaded nanocomposites were 1.95,

1.65, 1.70, and 1.48, respectively. The decrease in the magnitude of the peak loss factor is related to the immobilization of the rubber chains in the presence of nanofiller particles, indicating that the elastic nature of the nanocomposites was increased by the incorporation of nanoclay into the matrix (31).

Table 2. DMTA data of cured neat SR its nanocomposites with OC

| Sample	T_g (°C)	T_m (°C)	Tan δ_{max}
SR	-113.0	-51.4	1.95
SR-OC (1%)	-99.3	-52.3	1.65
SR-OC (2%)	-90.5	-53.8	1.70
SR-OC (3%)	-81.1	-43.4	1.48

AFM analysis of SR-OC bionanocomposites
Atomic force microscopy images of the samples based on neat SR and its corresponding nanocomposite containing 3 wt% OC are presented in Figures 2. In the case of neat SR, Figures 2a and b, which are 2-dimensional (2-D) and 3-dimensional (3-D) AFM images, show nearly uniform matrixes with small light regions that may arise from the soft segments, whereas the dark background with more high regions in the 2-D height micrograph of 3% SR–OC indicates the stiffer-layered silicate and that the particles are dispersed in the polymer matrix. This figure also shows evidence of OC particle aggregation in the polymer matrix (Fig. 2c).

The smoothness data of SR and its prepared nanocomposites are presented in Table 1. When the clay was incorporated, the RMS roughness and mean roughness values increased to 21.43±0.33 and 16.68±0.54 nm, respectively.

Effect of nanoclay on endothelial morphology
Figure 3 presents the change in SI, ө, and fractal dimension (FD) values for different OC loadings. Topological and fractal analyses showed rearrangement of the HUVECs caused by the OC nanolayers, exhibiting increased alignment with increased OC from 1 to 3 wt%. By increasing the OC ratio, the orientation angle increased gradually; however, the moderate growth observed in the SI curve was not statistically significant (*p > 0.05*). The most meaningful effect of clay incorporation was on fractals dimension (*p<0.05*). The highest morphological change occurred in 2% nanoclay, in which increases of 8.57% in orientation angle and 40.60% in cells SI were observed.
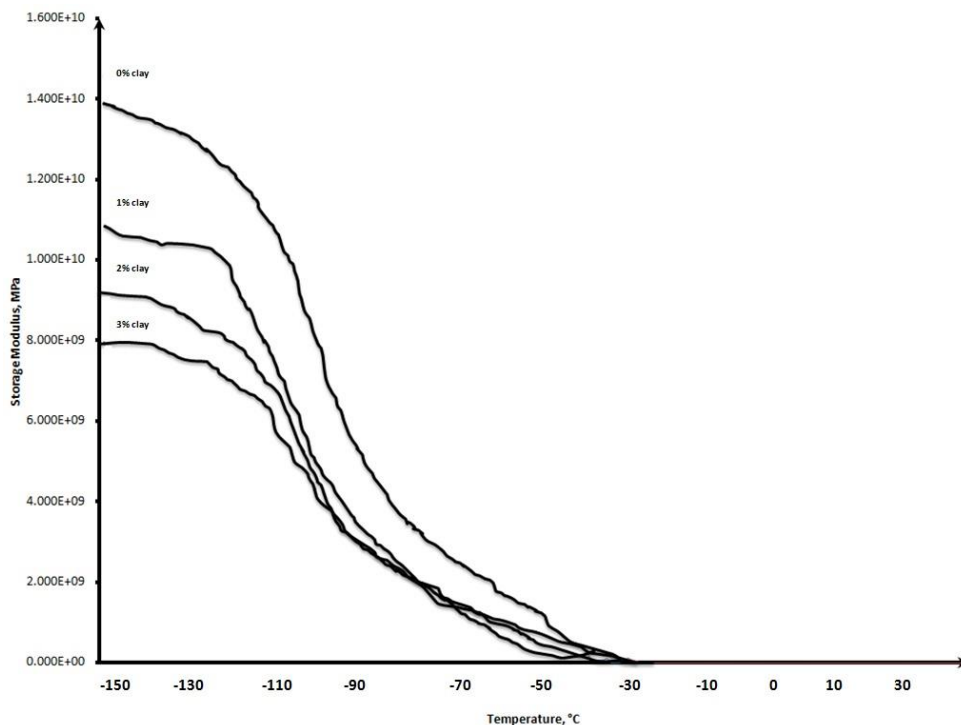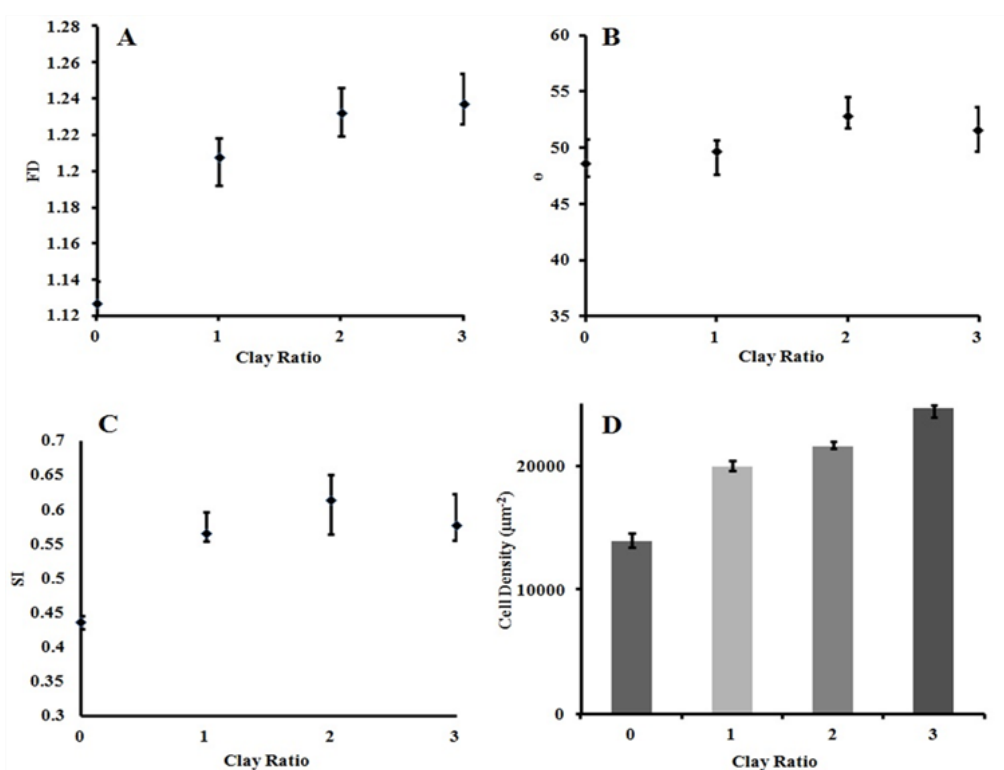

Fig. 1. Temperature dependence of the dynamic storage modulus for cured SR and SR/OC nanocomposites.
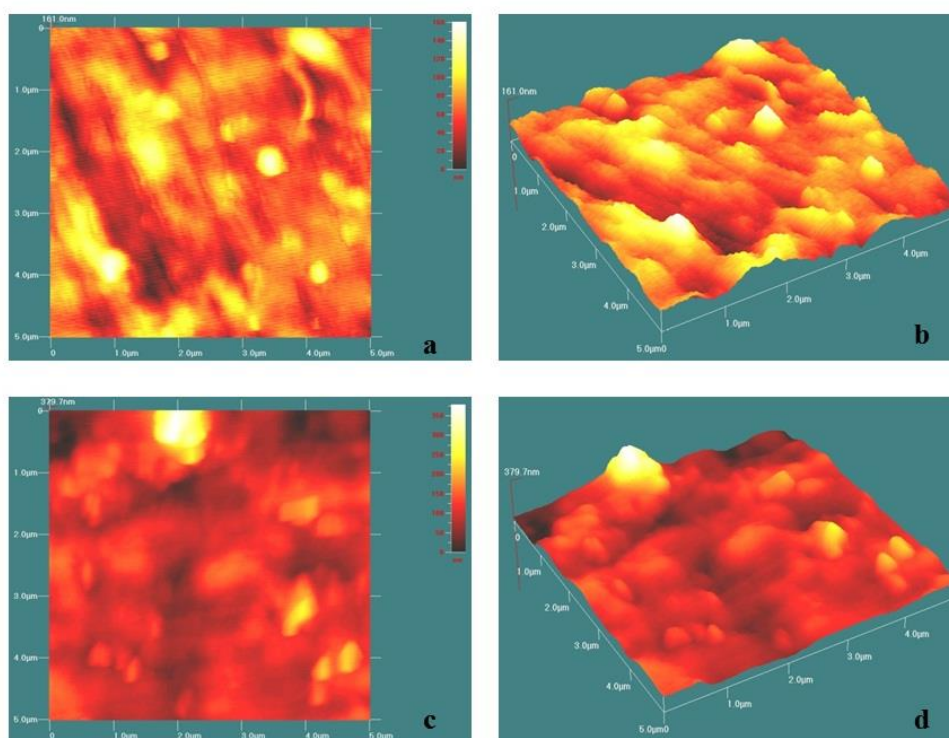
Fig. 2. 2D and 3D AFM micrographs for SR (a and b) and SR–OC (3%) substrates (c and d).


Fig. 3. Effects of OC incorporation on (a) FD, (b) θ, (c) SI, and (d) the relative cell density after 24 hours

Figure 3d represents the relative cell density for the different groups. The results indicated an increase in cell density with an increase of the mass ratio of nanofillers ($p<0.05$).

Detection of a matrix-degrading enzyme in HUVECs

The PMMP-2 was identified by gel zymography. This technique involves electrophoretic separation of proteins within polyacrylamide-gelatin sheets followed by enzymatic digestion of the gelatin within the sheets. Staining and de-staining of the sheets displays the activity of individual enzymes as color-free bands (Fig. 4).

The zymogram in Figure 4 reveals that the addition of OC filler increased HUVEC secretion of PMMP-2 into the culture medium following a 24-hour monolayer cell culture. The introduction of the nanoclay induced a significant increase in the intensity of the color-free band.
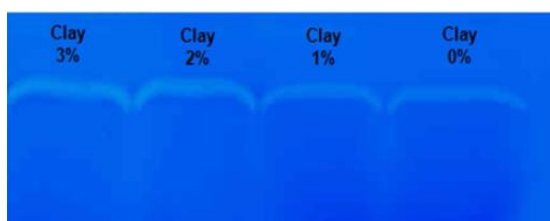
Fig. 4. Zymogram of protein lysates of HUVECs grown in 3, 2, 1, and 0% nanoclay on polyacrylamide-gelatin gels.

Discussion

One hypothesis proposes that the viscoelastic properties of cell substrates governs the cells' behavior (32). To understand the substrate-dependent cellular behavior of HUVECs, we prepared collagen-coated substrates based on SR, and corresponding nanocomposites with varying stiffness and roughness by adding small amounts of OC. The Young's modulus of composites ranged over 1 MPa. The molecular dynamic modulus of composites was lower than that of neat SR within the studied temperature range. This may be due to the slippage of the SR segments attached to the surface of the OC silicate layers as a result of low surface tension SR surface tension. Moreover, as shown in Figure 1, the inclusion of nanolayers onto the structure of SR led to the increase of the onset temperature for the decrease of storage modulus, indicating an interaction between the SR and OC nanolayers and an increase in T_g.

The fractal analysis is a useful tool for elucidating the effects of substrate viscoelasticity on cell behavior,

and one that may in the future become more widely used. The power of the model stems from the ease of microscopic imaging and data processing. Increase of FD as a measure of the increase in cell alignment and proliferation is in accordance with alterations in cell density due to high correlation factors. In other words, cell growth is the other factor, besides substrate viscoelasticity, that affects FD, leading to FD elevation due to the increase in the cell population. This means that although cell alignment leads to an increase in FD, the general rate of cell growth due to the presence of rough nanoparticles of clay in the SR surface reduces cell morphology complexity and the consequent FD value (33).

Cell proliferation in the SR-OC nanocomposites was greater than that in the SR sample. Cell morphology and the contact area of the HUVECs changed as the substrates' viscoelasticities changed. We conclude from the above results that the behavior of HUVECs is sensitive to the surface properties of the substrates to which they attach. It was also reasoned that not only the elastic modulus dictated by loading nanofillers could affect cell morphology, but also roughness might regulate cell proliferation. In the short term cultures, cells grown on rigid membranes became confluent more quickly than cells grown on soft membranes. This could be due to the mechanism by which cells spread on substrates and the contact areas, which are both directly related to the viscoelastic properties of substrates.

Matrix metalloproteinase is thought to play an important role in endothelial cell migration and matrix remodeling during various physiological and pathological processes. Here the data showed that HUVECs seeded on collagen-coated rigid and soft surfaces produced PMMP-2.

The surface viscoelasticity influenced the release of PMMP-2 on collagen-coated rigid substrata. The reason for the decreased degradability of the adsorbed proteins could be related to the lack of integrin clustering on soft SR substrata, changing the interaction between PMMP-2 and the cell membrane, thus enhancing PMMP-2 secretion (34, 35). Other causes of high PMMP-2 expression and subsequent ECM remodeling include the conformational changes in protein networks due to the stronger binding to the softer than the harder SR substrata (36, 37). Some literature has also correlated biocompatibility and the improved flexibility of the

designed substrate to the enhanced ability of cells to absorb and degrade the protein substrate (38, 39). Thus the data reported here support the hypothesis that the surface roughness and stiffness can predict cell fate including proliferation, migration, and differentiation.

Cell growth and alignment were enhanced in nanocomposite substrates. It has been shown that inorganic nanofillers have higher surface energies than polymer matrixes (40). Silicone rubber is hydrophobic due to the presence of methyl groups, and thus is considered a low surface energy polymer (41, 42). Increasing OC leads to a rise in the free surface energy by enhancing surface roughness (16).

Viscoelastic properties of substrates influence cell functions. Cytoskeletal arrangement and orientation are highly dependent upon mechanical and structural properties of the matrix such as elastic modulus, Poisson's ratio, and roughness (15, 16). When interacting with substrate, cellular responses, including relaxation time and adaptation by alterations in fibrous structures, are defined by local matrix deformability (20, 21). The adjustment of the cytoskeleton to the surface properties of the substrate is related to the polymerization and depolymerization of actin fibers (22), which act via focal adhesion proteins at the cell-substrate interface (20).

Our data demonstrates that surface roughness and stiffness are the two factors that govern cell behavior. Therefore, two principle conclusions can be drawn from our study; first, higher modulus materials influence endothelial cell adhesion and elongation, and

second, surface roughness influences cell spreading, the number of adhered cells, and integrin clustering.

Atomic force microscopy indicated that the surface profile of SR is composed of regular peaks and small, densely packed grains. In contrast, larger irregular peaks and deeper valleys were found in 3-D micrographs of SR-3% OC. Vascular endothelial cells were shown to preferentially align along the length of SR grains and decrease alignment as the grain depth increased due to the presence of layered silicate in the surface. The deeper valleys and wider grains have a greater effect on cell spreading and arrangement than alteration of the elastic modulus, and it was demonstrated that valley depth plays a leading role in contact guidance of endothelial cells on microtextured silicone elastomer. In other words, at lower grain widths and in shallower valleys, the modulus of the substrate seems to have the key role as compared with rough and different nanocomposite surfaces.

Conclusions

In conclusion, we applied a relatively simple method to fabricate a new type of bionanocomposite on which cell attachment, proliferation, and differentiation could be optimized by controlling the surface roughness and stiffness. Our study demonstrated that the viscoelastic properties of matrix surfaces have significant effects on cell behavior.

Acknowledgments

References

1. Cukierman E, Bassi DE, editors. Physico-mechanical aspects of extracellular matrix influences on tumorigenic behaviors. Semin Cancer biol; 2010 Jun;20(3):139-45.

2. Gentile F, Tirinato L, Battista E, Causa F, Liberale C, di Fabrizio EM, et al. Cells preferentially grow on rough substrates. Biomaterials. 2010 Oct;31(28):7205-12.

3. Slaughter BV, Khurshid SS, Fisher OZ, Khademhosseini A, Peppas NA. Hydrogels in regenerative medicine. Adv Mater. 2009 Sep;21(32-33):3307-29.

4. Zhang Y, Pang M, Xu Q, Lu H, Zhang J, Feng S. The curing retardation and mechanism of high temperature vulcanizing silicone rubber filled with superconductive carbon blacks. Polym Eng Sci. 2011 Jan;51(1):170-8.

5. Cortese B, Gigli G, Riehle M. Mechanical gradient cues for guided cell motility and control of cell behavior on uniform substrates. Adv Funct Mater. 2009 Sep;19(18):2961-8.

6. Lo C-M, Wang H-B, Dembo M, Wang Y-l. Cell movement is guided by the rigidity of the substrate. Biophys J. 2000 Jul;79(1): 144–52.

7. Guo W-h, Frey MT, Burnham NA, Wang Y-L. Substrate rigidity regulates the formation and maintenance of tissues. Biophys J. 2006 Mar;90(6):2213-20.

8. Frey MT, Tsai IY, Russell TP, Hanks SK, Wang Y-l. Cellular responses to substrate topography: role of myosin II and focal adhesion kinase. Biophys J. 2006 May;90(10):3774-82.

9. Teixeira AI, Ilkhanizadeh S, Wigenius JA, Duckworth JK, Inganäs O, Hermanson O. The promotion of neuronal maturation on soft substrates. Biomaterials. 2009 Sep;30(27):4567-72.

10. Ulrich TA, de Juan Pardo EM, Kumar S. The mechanical rigidity of the extracellular matrix regulates the structure, motility, and proliferation of glioma cells. Cancer Res. 2009 May;69(10):4167-74.

11. Cavalcanti-Adam EA, Volberg T, Micoulet A, Kessler H, Geiger B, Spatz JP. Cell spreading and focal adhesion dynamics are regulated by spacing of integrin ligands. Biophys J. 2007 Apr;92(8):2964-74.

12. Nicolas A, Safran SA. Limitation of cell adhesion by the elasticity of the extracellular matrix. Biophys J. 2006 Jul;91(1):61-73.

13. Zamir E, Geiger B. Molecular complexity and dynamics of cell-matrix adhesions. J Cell Sci. 2001 Oct;114(Pt 20):3583-90.

14. Berrier AL, Yamada KM. Cell–matrix adhesion. J Cell Physiol. 2007 Dec;213(3):565-73.

15. De R, Zemel A, Safran SA. Dynamics of cell orientation. Nat Phys. 2007 Jul;3(9):655-9.

16. Wei Z, Deshpande VS, McMeeking RM, Evans AG. Analysis and interpretation of stress fiber organization in cells subject to cyclic stretch. J Biomech Eng. 2008 Jun;130(3):031009.

17. Wang H-B, Dembo M, Wang Y-L. Substrate flexibility regulates growth and apoptosis of normal but not transformed cells. Am J Physiol Cell Physiol. 2000 Nov;279(5):C1345-50.

18. Iwanaga Y, Braun D, Fromherz P. No correlation of focal contacts and close adhesion by comparing GFP-vinculin and fluorescence interference of DiI. Eur Biophys J. 2001;30(1):17-26.

19. Qian J, Gao H. Soft matrices suppress cooperative behaviors among receptor-ligand bonds in cell adhesion. PLoS One. 2010 Aug;5(8):e12342.

20. De R, Safran SA. Dynamical theory of active cellular response to external stress. Phys Rev E Stat Nonlin Soft Matter Phys. 2008 Sep;78(3 Pt 1):031923.

21. Hsu H-J, Lee C-F, Kaunas R. A dynamic stochastic model of frequency-dependent stress fiber alignment induced by cyclic stretch. PLoS One. 2009;4(3):e4853.

22. Nekouzadeh A, Pryse KM, Elson EL, Genin GM. Stretch-activated force shedding, force recovery, and cytoskeletal remodeling in contractile fibroblasts. J Biomech. 2008 Oct;41(14):2964-71.

23. Ma J, Yu ZZ, Kuan HC, Dasari A, Mai YW. A new strategy to exfoliate silicone rubber/clay nanocomposites. Macromol Rapid Commun. 2005 May;26(10):830-3.

24. Razavi Nouri M, Hay JN. Time-temperature superposition and dynamic mechanical properties of metallocene polyethylenes. Iran Polym J. 2004;13:363-70.

25. Barick AK, Tripathy DK. Effect of organoclay on thermal and dynamic mechanical properties of novel thermoplastic polyurethane nanocomposites prepared by melt intercalation technique. Polym Advan Technol. 2010 Dec;21(12):835-47.

26. Maiti M, Bhowmick AK. New insights into rubber–clay nanocomposites by AFM imaging. Polymer. 2006 Aug;47(17):6156-66.

27. Haghighipour N, Tafazzoli-Shadpour M, Shokrgozar MA, Amini S. Effects of cyclic stretch waveform on endothelial cell morphology using fractal analysis. Artif Organs. 2010 Jun;34(6):481-90.

28. Zhang L, Kahn CJ, Chen H-Q, Tran N, Wang X. Effect of uniaxial stretching on rat bone mesenchymal stem cell: orientation and expressions of collagen types I and III and tenascin-C. Cell Biol Int. 2008 Mar;32(3):344-52.

29. von Offenberg Sweeney N, Cummins PM, Birney YA, Cullen JP, Redmond EM, Cahill PA. Cyclic strain-mediated regulation of endothelial matrix metalloproteinase-2 expression and activity. Cardiovasc Res. 2004 Sep;63(4):625-34.

30. Jena KK, Narayan R, Raju KV. Investigation of the effect of ZnO nanoparticles on the thermomechanical and microbial properties of hyperbranched polyurethane-urea hybrid composites. Polym Int. 2012 Aug;61(8):1309-17.

31. Kruenate J, Tongpool R, Kongrat P. Rheological Characteristics of Ethylene Vinyl Acetate (EVA)/Silane Nanocomposites. J Metast Nanocryst Mater. 2005 Jan;23:227-30.

32. Nemir S, West JL. Synthetic materials in the study of cell response to substrate rigidity. Ann Biomed Eng. 2010 Jan;38(1):2-20.

33. Goli-Malekabadi Z, Tafazzoli-Shadpour M, Rabbani M, Janmaleki M. Effect of uniaxial stretch on morphology and cytoskeleton of human mesenchymal stem cells: static vs. dynamic loading. Biomed Tech (Berl). 2011 Oct;56(5):259-65.

34. Cretel E, Pierres A, Benoliel A-M, Bongrand P. How cells feel their environment: a focus on early dynamic events. Cell Mol Bioeng. 2008 Mar;1(1):5-14.

35. Paszek MJ, Boettiger D, Weaver VM, Hammer DA. Integrin clustering is driven by mechanical resistance from the glycocalyx and the substrate. PLoS Comput Biol. 2009 Dec;5(12):e1000604.

36. Kumar CS, Mande SC. Protein chaperones and non-protein substrates: on substrate promiscuity of GroEL. Curr Sci (Bangalore). 2011 Jun;100(11):1646-53.

37. Meireles L, Gur M, Bakan A, Bahar I. Pre-existing soft modes of motion uniquely defined by native contact topology facilitate ligand binding to proteins. Protein Sci. 2011 Oct;20(10):1645-58.

38. Hannachi Imen E, Nakamura M, Mie M, Kobatake E. Construction of multifunctional proteins for tissue engineering: Epidermal growth factor with collagen binding and cell adhesive activities. J Biotechnol. 2009 Jan;139(1):19-25.

39. Wang H-J, Di L, Ren Q-S, Wang J-Y. Applications and degradation of proteins used as tissue engineering materials. Materials. 2009 May;2(2):613-35.

40. Tian M, Cheng L, Zhang L. Interface and mechanical properties of peroxide cured silicate nanofiber/rubber composites. J Appl Polym Sci. 2008 Oct;110(1):262-9.

41. Ataeefard M, Moradian S. Surface properties of polypropylene/organoclay nanocomposites. Appl Surf Sci. 2011 Jan;257(6):2320-6.

42. Haji K, Zhu Y, Otsubo M, Honda C. Surface modification of silicone rubber after corona exposure. Plasma Process Polym. 2007 Apr;4(S1):S1075-S80.